

Optimization of S-Shaped Fin Channels in a Printed Circuit Heat Exchanger for Supercritical CO₂ Test Loop

Xiaoqin Zhang, Xiaodong Sun, Richard N. Christensen

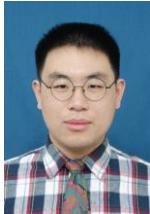
The Ohio State University
201 W. 19th Avenue, Columbus, OH 43210
zhang.3836@osu.edu; sun.200@osu.edu; christensen.3@osu.edu

Mark Anderson

University of Wisconsin-Madison
1415 Engineering Drive, Madison, WI 53706
manderson@engr.wisc.edu

Matt Carlson

Sandia National Laboratories
P.O. Box 5800, Albuquerque, NM 87185-1136
mcarlo@sandia.gov



Xiaoqin Zhang

2013, B.S. in Nuclear Engineering, Shanghai Jiao Tong University, Shanghai, China

2013 – Present, Graduate Research Associate, The Ohio State University

ABSTRACT

The S-shaped fin channels were proposed in the literature to address the pressure drop reduction issue in the design of printed circuit heat exchangers (PCHEs) for application of supercritical CO₂ (s-CO₂) Brayton cycles. To investigate the thermal-hydraulic characteristics of S-shaped fin channels, an s-CO₂ test loop is being constructed at The Ohio State University for testing prototypic PCHEs with S-shaped fin channels. To maximize the heat exchanger thermal effectiveness and minimize the overall pressure drop across the heat exchanger core, a shape optimization of S-shaped fin channels was carried out using a surrogate model of a second-order response surface methodology based on CFD simulations of nine S-shaped fin design models. One of the widely used multi-objective evolutionary algorithms, NSGA-II, was adopted in the optimization process. The selected shape factors for the S-shaped fin channels optimization are the fin angle and fin length. The optimization results indicate that the small-fin-angle channels with large fin length are able to reduce the pressure drop while the large-fin-angle channels with small fin length are favorable in increasing the heat exchanger thermal effectiveness.

1. Introduction

Supercritical carbon dioxide ($s\text{-CO}_2$) Brayton cycle, compared with the conventional steam Rankine cycle and other gas Brayton cycles, has been recognized as one of the most promising power conversion systems for high-temperature gas-cooled reactors (HTGRs). In such an indirect power cycle system, intermediate heat exchangers (IHXs) are used to transfer the heat of the primary helium flow from the reactor core to the secondary fluid, i.e., $s\text{-CO}_2$. Compact heat exchangers (CHEs), which are widely used in the chemical and petroleum refining industries, are considered as a promising candidate for IHXs in the advanced nuclear reactor concepts.

CHEs are usually characterized by high compactness achieved by fins or mini and micro flow channels, which can lead to heat transfer enhancement with considerable size reduction. One of the promising CHE candidates as IHXs in advanced reactor and gas turbine systems is the printed circuit heat exchangers (PCHEs), which typically have a surface area density as high as $2,500 \text{ m}^2/\text{m}^3$ [1]. Furthermore, PCHEs are able to withstand extremely high temperatures and high pressures, possibly up to 900°C and 50 MPa. Originally developed and manufactured by Heatric, PCHEs are formed by diffusion bonding metal plates in which flow channels are photochemically etched. To date, a number of flow channels have been proposed for PCHEs, including straight, zigzag, S-shaped fin, and airfoil fin channels, as shown in Fig. 1. In this study, we focus on the thermal-hydraulic characteristics of PCHEs with S-shaped fin flow channels, which are also called sinusoidal fin flow channels in literature.



Figure 1. Four PCHE Surfaces: Straight, Zigzag, S-shaped Fin and Airfoil Fin Channels (Left to Right).

In 2007, Tsuzuki et al. [2] in the Tokyo Institute of Technology (TIT) for the first time introduced a new surface geometry concept, i.e., S-shaped fin concept. This newly proposed surface geometry was based on zigzag or wavy-sinusoidal channels. The development of the S-shaped fins from conventional zigzag channels is shown in Fig.2. In 2009, Tsuzuki et al. [3] carried out a parametric study on the shape of the S-shaped fin channels through three-dimensional computational fluid dynamics (3D-CFD) simulations. Several factors that could affect the pressure drop and heat transfer performance were discussed, including the fin angle, fin width, fin length, and edge roundness. Guidance for the S-shaped fin design was provided. Experimentally, a PCHE with S-shaped fin channels was tested in a supercritical carbon dioxide loop, and the comparison of thermal-hydraulic performance was made in terms of the pressure drop factor and Nusselt number [4]. It was found that with the same geometrical parameters, the PCHE with the S-shaped fin channels showed 4-5 times less in the pressure-drop factor than the one with the zigzag channels. However, the Nusselt number was also 24-34% smaller. The experimentally-developed correlations for the S-shaped-fin PCHEs were provided.

The configuration of the S-shaped fin channels is very similar to the conventional zigzag channels. The staggered pattern can repeatedly disturb the developed thermal boundary layers along the wall, thus enhancing the heat transfer. In addition, the unique offset configuration of the S-shaped fins can effectively reduce the additional pressure drop of swirl flows, reversed flows, and eddies that are formed around bend corners in the zigzag channels [2]. The advantages of the discontinuous islanded sinusoidal fins can be further maximized by a shape optimization, which was the original motivation for this study. In this case, a reference PCHE with the S-shaped fin channels was identified, and CFD simulations of nine S-shaped fin design models were carried out using ANSYS-Fluent to find an optimized design.

The shape optimization in terms of the overall thermal-hydraulic performances of a PCHE can be carried out using the multi-objective evolutionary algorithms (MOEA). A similar approach was utilized by Lee et al. [5], who optimized a double-faced type PCHE with zigzag channels. One of the popular MOEAs is the non-dominated sorting genetic algorithms (NSGA-II) [6]. This method is able to search a set of well-distributed Pareto-optimal solutions quickly and accurately. To correlate the S-shaped fins' geometrical parameters to the thermal-hydraulic characteristics, a surrogate model was developed using the response surface methodology (RSM) [7]. A second-order RSM was adopted to develop the surrogate model based on CFD-simulation results of nine different S-shaped fin designs, which are obtained through Latin hypercube sampling (LHS).

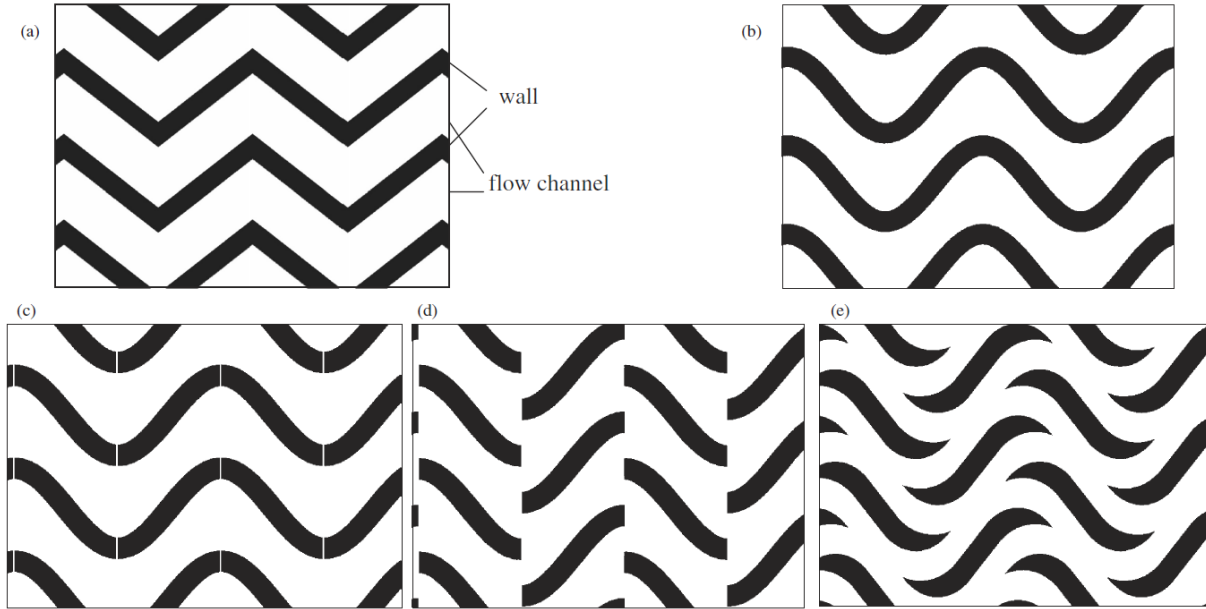


Figure. 2. Development of S-shaped Fin Channels: (a) Zigzag Channels; (b) Wavy-Sinusoidal Channels; (c) Bends Cut; (d) Off-set Shifting; (e) S-shaped Fin Channels with Tips Elongation [3].

The reference S-shaped fin PCHE for thermal-hydraulic analysis is actually identified to be the one that is designed for testing in the Thermal-Hydraulic Laboratory at The Ohio State University. It is designed as a scaled-down IHX prototype used in helium to s-CO₂ reactor and power conversion systems, as shown in Fig. 3. The PCHE's hot side is the zigzag channel while the cold side is the S-shaped fin channel. It will be tested on a facility consisting of an existing loop, i.e., the high-temperature helium facility (HTHF), and an s-CO₂ test loop (STL) that is currently being constructed, as shown in Fig. 3. The experimental test will be performed to investigate both the zigzag and S-shaped fin channels' thermal hydraulics. The design of the S-shaped-fin-channel plate is shown in Fig. 4. The operating conditions for the reference S-shaped fin PCHE are listed in Table I.

Table I. Operating Condition of a Prototypic Zigzag-S-Shaped-Fin PCHE

Item	Primary side	Secondary side
Working fluids	Helium	s-CO ₂
Mass flow rate, kg/h	33.1	230.0
Pressure, MPa	2.0	15.0
Inlet temperature, °C	730.0	418.8
Outlet temperature, °C	452.1	589.4

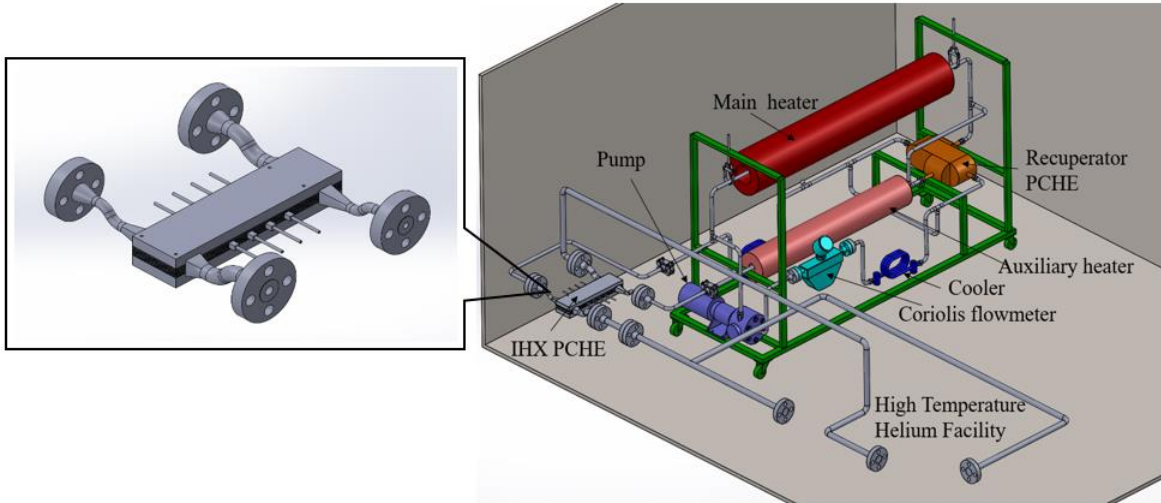


Figure. 3. Schematic of the Reference Prototypic IHX PCHE (Left) and the s-CO₂ Test Loop (Right).

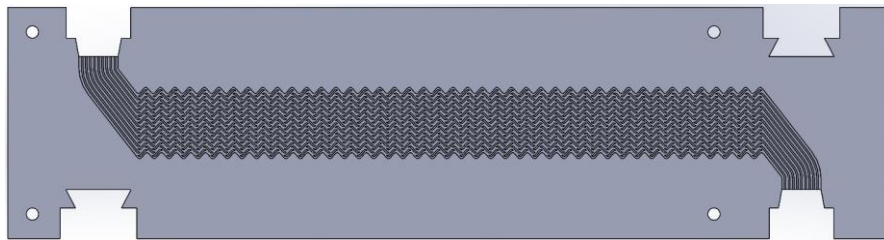


Figure. 4. The S-shaped Fin Channel Plate in the Prototypic IHX PCHE.

2. Geometrical Characteristics of S-Shaped Fins

The reference S-shaped fin channels are designed based on the S-shaped-fin PCHE that was tested in TIT [4]. The detailed information of the geometrical parameters can be found in Fig. 5 and Table II.

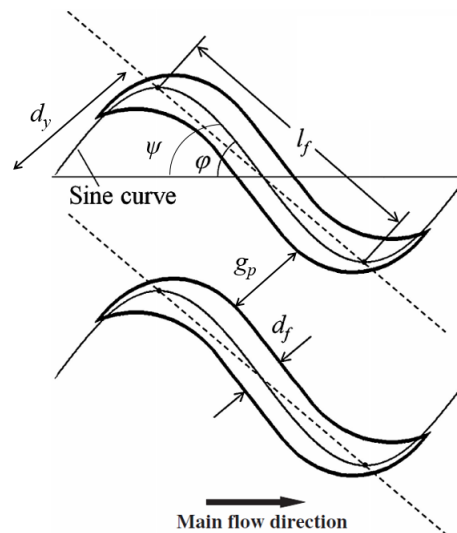


Figure. 5. Schematic of S-shaped Fin Surface Geometrical Characteristics [3].

Table II. S-shaped Fin Surface Geometrical Parameters [4]

Parameters	Values
Plate thickness, t_p , mm	1.5
Fin angle, φ , °	52
Fin length, l_f , mm	4.8
Fin width, d_f , mm	0.8
Hydraulic diameter, D_h , mm	1.629
Fin pitch in x-/y-direction, p_x/p_y , mm	7.442/3.483
Fin height, h_s , mm	0.94

The equation-based curves that constitutively form the shape of the S-shaped fins are defined by the fin length l_f , fin angle φ , and fin width d_f . The periodically-staggered pattern is determined by the longitudinal pitch p_x and the transverse pitch p_y . The sinusoidal curve can be expressed by

$$y = \xi \sin(\omega x). \quad (1)$$

The relationships between the geometrical parameters and ξ , ω are shown as follows:

$$\xi = \frac{1}{2} l_f \sin \psi, \quad (2)$$

$$\omega = \frac{\pi}{l_f \cos \psi}, \quad (3)$$

where the pitch angle ψ can be obtained from:

$$\frac{\pi}{2} \tan \psi = \tan \varphi. \quad (4)$$

The S-shaped fin can be formed by shifting the sinusoidal curve along a direction vector (a, b) , which can be computed by

$$a = \frac{d_f \cos \beta}{2 \cos \left(\frac{\pi}{2} - \varphi - \beta \right)}, \quad (5)$$

$$b = \frac{d_f \sin \beta}{2 \cos \left(\frac{\pi}{2} - \varphi - \beta \right)}, \quad (6)$$

where β is the direction vector angle with respect to the x -axis. It is a user-defined parameter that controls the arc length of the fin tips. Different values of β will result in a different shape of S-shaped fins, which also affects the thermal-hydraulic characteristics. Generally, a large direction vector angle leads to a long arc of the fin tip. For some S-shaped fins' shapes with small fin length and fin angle, β needs to be sufficiently small such that a sinusoidal fin shape can be formed.

The transverse pitch p_y is dependent on the fin gap g_p , which is further dependent upon the fin height H_f (also referred to as the channel depth) and the fin width d_f due to the mechanical strength requirement. In the mechanical analysis, two neighboring S-shaped fins are assumed to be treated as two ridges for a typical zigzag channel. It is recommended to use the eq. (7) for a simplified mechanical analysis to determine the zigzag channel's ridge thickness $d_{f,zz}$ [8]:

$$d_{f,zz} = \left(\frac{\Delta p}{\sigma_D} \right) g_p, \quad (7)$$

where Δp and σ_D are the pressure differential between plates and the maximum allowable stress of the plate base material, respectively. Therefore, we can use the same equation to determine the fin gap g_p :

$$g_p = \left(\frac{\sigma_D}{\Delta p} \right) d_{f,ss}. \quad (8)$$

The neighboring fin distance d_y can then be obtained as follows:

$$d_y = d_f + g_p. \quad (9)$$

Therefore, we can calculate p_x and p_y by

$$p_x = 2l_f \cos \psi, \quad (10)$$

$$p_y = d_y / \cos \psi. \quad (11)$$

As the etching process usually creates a semi-circular cross-sectional profile, it is reasonable to assume that the fin height is only half of the fin gap, i.e.,

$$H_f = \frac{1}{2} g_p. \quad (12)$$

Therefore, we can conclude that the geometrical characteristics of the S-shaped fin channels can be defined by the fin angle, fin length, fin height and fin width. The latter two parameters are actually dictated by the required mechanical strength. As analyzed in a previous study [9], the reference S-shaped fin model was simulated with prescribed mechanical loading, showing reliable structural integrity under a pressure differential up to 15 MPa. Accordingly, the fin height and fin width will be identical to those in the reference model.

It is noted that the tips' roundness and the arc length of guide wings in the S-shaped fin channels also play an important role in the thermal-hydraulic performances. However, the roundness radius is difficult to be controlled in the current etching technique, since the S-shaped fins' width is in the length scale of 1 mm. The tips may be completely etched away in some cases. In this study, the roundness radius is recommended to be 0.1 mm [3]. Regarding the arc length, it is essentially dictated by the direction vector angle, and in some particular S-shaped fin designs with extremely small fin angle and small fin length, it is even impossible to form the S-shaped fin by shifting the sinusoidal curves. For a simplified analysis, the direction vector angle is defined to be 10° and the effect of the arc length will not be studied in this paper.

3. Numerical Studies

Numerical studies were carried out to investigate the thermal-hydraulics of the various designs of S-shaped fin channels. Due to the periodic nature of S-shaped fin channels, a computational model consisting of two rows of fins that are periodic in both x - and y -direction, as shown in Fig. 6, is selected to reduce the computational cost in CFD simulations. There are 13 plus 2 halves of solid fins in the conjugate heat transfer model. Three plates sandwich both hot and cold fluid flow domains. The boundary conditions are all set to be periodic except the inlets and outlets as well as the front and rear adiabatic walls. Therefore, the computational domain can simulate an infinitely large core without any wall effects. The actual dimensions of the computation model are specified by the particular study case.

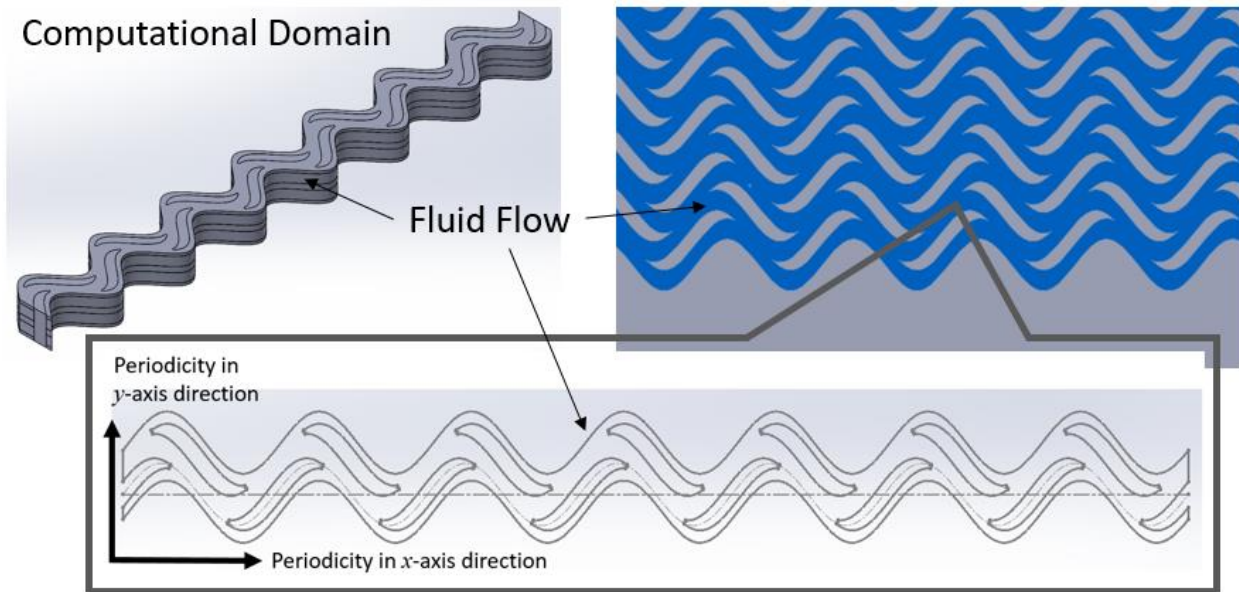


Figure. 6. The Periodicity of the Computational Domain.

Besides the CFD simulation of the reference model, 9 cases were also simulated, which were selected by Latin hypercube sampling in terms of two design variables, i.e., the fin angle and fin length. Fig. 6 shows the surface geometry of S-shaped fin channels in the 9 cases. The detailed information is listed in Table III. In these models, the fin height and fin width were specified to be 0.94 mm and 0.8 mm, respectively. The direction vector angle is chosen to be 10° , as explained in the previous section. The distribution of the samplings is also shown in Fig. 7. It should be noted that the cases with extremely small fin angle and fin length often result in difficulties in CAD modeling. Consequently, the sampling space is defined to be $10 - 60^\circ$ for the fin angle and 4 - 16 mm for the fin length.

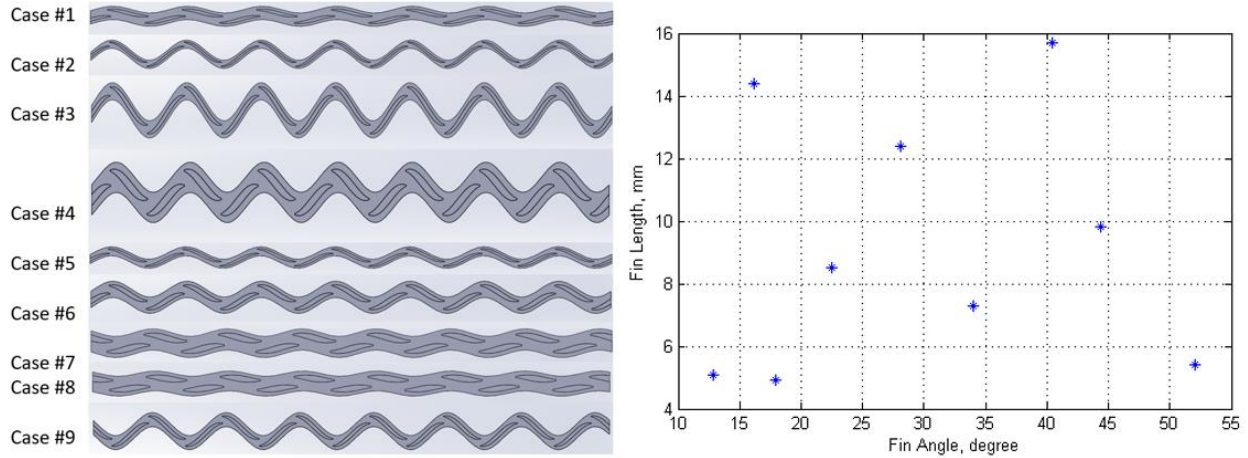


Figure. 7. The S-shaped Fin Simulation Model of 9 Cases and the Distribution in the Design Space.

Table III. Geometrical Parameters of 9 Cases of S-shaped Fin Design.

Case	ϕ	l_f	ψ	ζ	ω	a	b	p_x	p_y
Units	degree	mm	degree	mm	mm-1	mm	mm	mm	mm
1	16.17	14.45	10.46	1.311	0.221	1.34	0.24	28.36	5.04
2	40.43	15.74	28.48	3.750	0.227	0.51	0.09	27.62	3.05
3	22.50	8.50	14.78	1.084	0.382	0.73	0.13	16.44	2.77
4	51.97	5.45	39.15	1.719	0.743	0.45	0.08	8.45	3.45
5	28.15	12.38	18.82	1.995	0.268	0.64	0.11	23.46	2.83
6	34.02	7.26	23.26	1.432	0.471	0.57	0.10	13.33	2.92
7	17.86	4.92	11.60	0.494	0.652	0.84	0.15	9.63	2.74
8	12.87	5.13	8.28	0.369	0.619	1.46	0.13	10.15	2.70
9	44.37	9.84	31.93	2.600	0.376	0.48	0.09	16.70	3.16

Tsuzuki et al. [3] performed a parametric study on the shape of the S-shaped fins using 3D-CFD simulation. Three turbulence models in the Fluent code were used to compare with the experimental results. It was recommended to use k- ϵ RNG model due to the relatively more accurate heat transfer calculations than other k- ϵ models. In the current studies, both k- ϵ and k- ω turbulence models were used in the CFD simulation using ANSYS-Fluent. It was found that k- ω models were difficult to obtain converged results while the simulation of k- ϵ models was able to converge with the relaxation factor reduced. One of the possible reasons for that phenomenon can be the inappropriate uniform pressure outlet boundary conditions. The velocity field at the middle cross-sections of the S-shaped fins is not uniform due to the presence of neighboring fins, thus creating pressure gradients at those cross-sections. Therefore, it is possible that some turbulence models will fail because of the uniform outlet pressure boundary condition specified in the simulation. As to the k- ϵ models, the results showed that there was no obvious difference between k- ϵ RNG and k- ϵ Realizable model. Eventually, we chose the k- ϵ Realizable model for more stable convergence.

Four meshing schemes were tested for mesh independence study in the reference model, as listed in Table IV. All parts in the computational model use sweep meshing method to reduce the overall number

of element. Since the fluid flow contacts the solid fin walls as well as the top and bottom plate walls, the cells adjacent to the solid fin walls are inflated with 10 layers while the cells close to the top and bottom walls are biased meshed in sweeping direction, as shown in Fig. 8. It was found that the difference in the heat transfer performances between the medium-fine and fine meshing schemes is negligible while the difference of the pressure drops is less than 1%. Therefore, the medium-fine mesh is chosen.

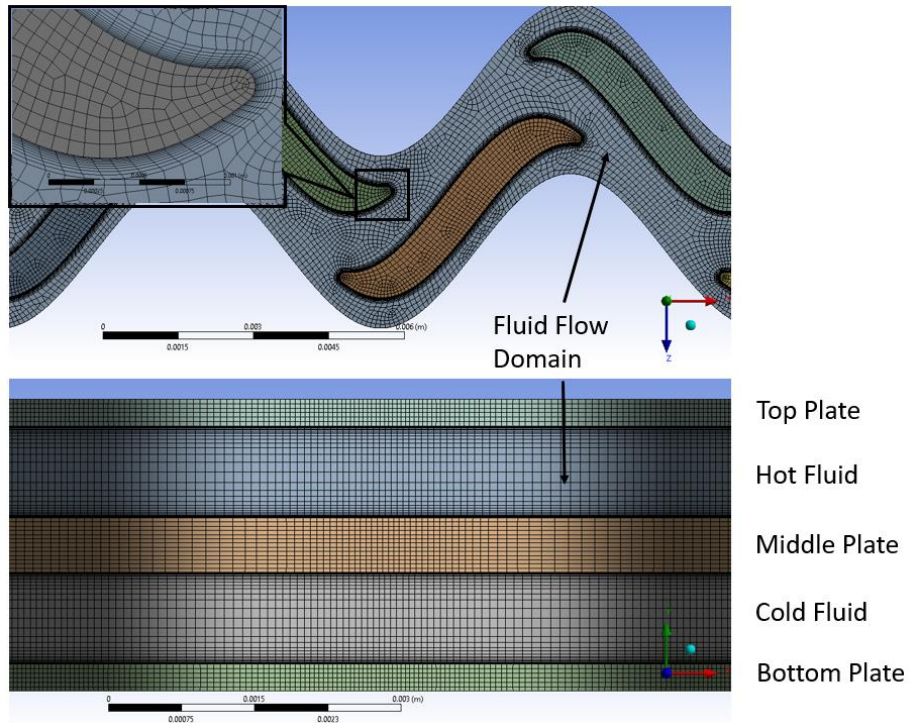


Figure. 8. The Meshing Scheme for Both Fluid and Solid Computational Domain.

Table IV. Mesh Independence Study

Description	Mesh Elements in Fluid Flow Domain	Pressure Drop (kPa)	Relative Deviation
Coarse	1,568,330	82.385	5.68%
Medium	2,697,300	79.747	2.30%
Medium-Fine	4,856,300	78.352	0.51%
Fine	6,253,150	77.956	0.00%

For the simulations of 9 cases, polynomial functions of the $s\text{-CO}_2$ thermo-physical properties were used for the temperature range of 150 to 700°C and the system pressure of 15 MPa. The data were retrieved from the NIST Webbook (National Institute of Standards and Technology) [10]. The base material was selected to be alloy 617, the same as the one used in the prototypic PCHE.

A pressure drop factor, defined as the pressure drop per unit length, can be used to analyze the pressure drop characteristics, which is defined as follows:

$$\delta P = \frac{P_1 - P_2}{L_{12}}. \quad (13)$$

This pressure drop factor does not currently involve Reynolds number dependence. All of the simulations assume a fixed Reynolds number of typical 20,000. Therefore, the mass flow rate is accordingly adjusted. The subscript 1 and 2 denote the selected locations of the area-averaged gauge pressure. The global heat transfer coefficient is calculated as

$$h = \left| \frac{Q}{A_s(T_w - T_b)} \right|. \quad (14)$$

Because of the complexity of the S-shaped fin's geometry, it is difficult to obtain an averaged local heat transfer coefficient. Therefore, the temperature difference between the wall and the bulk fluid is defined to be half of the logarithmic mean temperature difference (LMTD). The simulation results of 9 cases are listed in Table V.

Table V. Simulation Results of 9 Cases of S-shaped Fin Designs.

Case	$T_{c,in}$	$T_{h,in}$	$T_{c,out}$	$T_{h,out}$	$P_1 - P_2$	δP	h
Unit	K	K	K	K	kPa	kPa/mm	W/m ² -K
1	675	875	804.4	747	6.21	0.044	3245.0
2	675	875	821.7	729.7	15.62	0.113	3638.2
3	675	875	793.1	758.7	8.16	0.099	4067.5
4	675	875	787.9	764.7	13.22	0.313	4384.8
5	675	875	810.7	740.8	11.89	0.101	3922.4
6	675	875	791.8	759.9	8.26	0.124	3321.8
7	675	875	767.5	784.2	5.58	0.116	4379.4
8	675	875	766.3	785.5	5.03	0.103	4085.5
9	675	875	805.7	745.9	11.74	0.141	3842.7

4. Shape Optimization of the S-shaped Fin Channels

Based on the simulation results, it is possible to perform a shape optimization of the S-shaped fin channels for the application to the reference PCHE. As discussed beforehand, the design variables are the fin angle and fin length, as these two factors are critical to the thermal-hydraulic performances of the S-shaped fin channels. The design space is identical to the sampling space. The objective functions are selected to the test PCHE thermal effectiveness and the pressure drop across the core. Regarding the thermal modeling of the test PCHE, various design models of the S-shaped fin channels are used in the evaluation of the two objective functions, where the pressure drop and heat transfer coefficient are calculated using a surrogate model. It is noted that since there is no Reynolds number dependence in the developed surrogate model. For the reference PCHE, the number of S-shaped fin channels and the core length of the heat exchanger are pre-defined. A second order RSM surrogate model is developed based on the simulation results, which can be expressed by [7]:

$$y = \beta_0 + \sum_{j=1}^k \beta_j x_j + \sum_{j=1}^k \beta_{jj} x_j^2 + \sum_{i < j=2}^k \sum_{i=1}^k \beta_{ij} x_i x_j \quad (15)$$

where x , y and β are the design variables, dependent variables, and RSM coefficients, respectively. The calculated coefficients are listed in Table VI. Note that since the heat transfer area and hydraulic diameter of S-shaped fin channels are difficult to be calculated directly from the geometrical parameters, the corresponding surrogate models for the hydraulic diameter and heat transfer area are also developed as well. Figure 9 and 10 show the thermal-hydraulic dependence on the fin angle and fin length using the surrogate model.

Table VI. Coefficients of RSM Surrogate Model.

Description	Heat transfer area	Hydraulic diameter	Pressure drop per unit length	heat transfer coefficient
symbol	A_s	D_h	δP	h
β_0	6.511	1.170	1.391×10^{-1}	5.084×10^3
β_1	-6.175×10^{-2}	4.824×10^{-3}	9.751×10^{-3}	-1.033×10^3
β_2	-2.802×10^{-1}	6.114×10^{-2}	-5.948×10^{-2}	4.682×10^2
β_3	7.527×10^{-2}	5.921×10^{-5}	1.369×10^{-2}	1.932×10^2
β_4	9.338×10^{-2}	-1.263×10^{-2}	4.306×10^{-2}	7.636×10
β_5	-5.417×10^{-2}	1.121×10^{-3}	-4.154×10^{-2}	-2.064×10^2

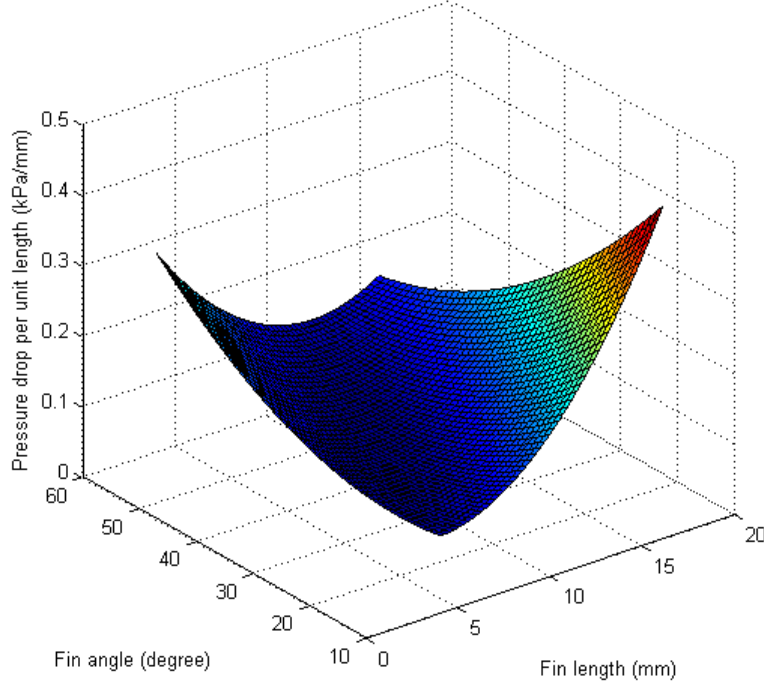


Figure. 9. The Pressure Drop Dependence based on the Surrogate Model

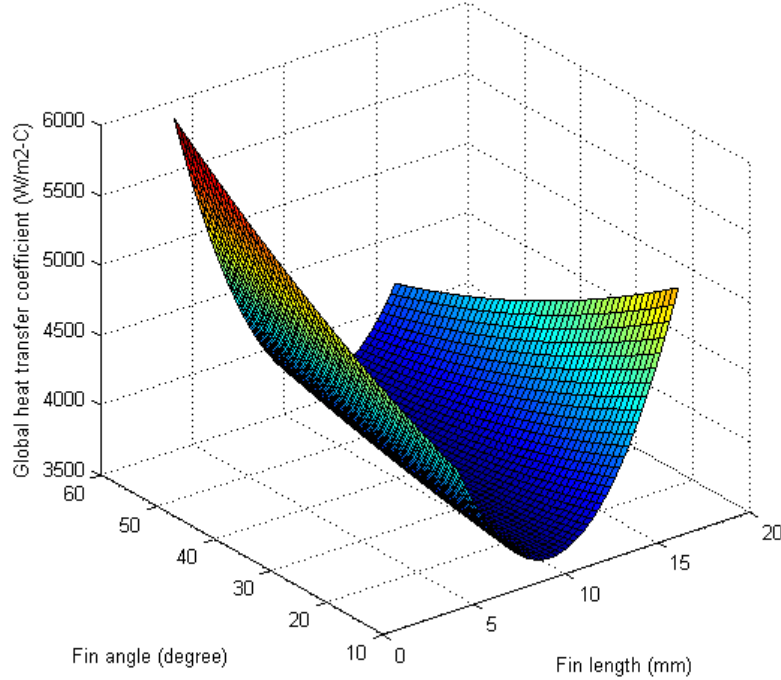


Figure. 10. The Heat Transfer Coefficient Dependence based on the Surrogate Model

With respect to the pressure drop across the heat exchanger core, it can be calculated through the pressure drop factor and the heat exchanger core length. Regarding the heat exchanger thermal effectiveness, a counter-flow ϵ -NTU method is adopted. With the assumption of a simple slab heat conduction model between the hot and cold sides using the mean plate thickness t_o , the overall heat transfer coefficient U can be calculated by [11]:

$$\frac{1}{U_h A_{s,h}} = \frac{1}{U_c A_{s,c}} = \frac{1}{h_h A_{s,h}} + \frac{t_w}{k_w A_{s,w}} + \frac{1}{h_c A_{s,c}} \quad (16)$$

One of the popular MOEAs, NSGA-II, is used in the shape optimization. The detailed procedure of the optimization method can be referred to Ref. [6]. An in-house NSGA-II code was developed to optimize the design of an IHX PCHE with zigzag channels [12]. In the current study, it was used to optimize the shape of S-shaped fins in terms of the evaluation of both the heat exchanger core pressure drop and thermal effectiveness.

Figure. 11 shows the entire solution space with 5,000 sampled S-shaped fin designs. It can be observed from the distribution of the solutions that generally the heat exchanger core pressure drop increases as the heat exchanger thermal effectiveness increases. This is consistent with the expectation that the minimization of the pressure drop and the maximization of the heat transfer performance are usually conflicting with each other. Figure. 11 also shows the Pareto-optimal solutions using the NSGA-II algorithm and the corresponding clustered solutions, which are listed in Table VII. Figure. 12 shows the distribution of the fin angle and the fin length for all of the Pareto-optimal solutions. It indicates that the optimized designs can be divided into two groups: the low-angle-fin group and the high-angle-fin group. In the low-angle-fin group, the small-angle S-shaped fins are able to reduce the pressure drop since small angles streamline the flow and mitigate the flow stagnation that is usually found at the tips of fins. Long fins are

also favorable in pressure drop reduction since the flow can be stabilized through long fin channels. However, the thermal effectiveness is decreased for long fins because the thermal boundary layer is developed through long fin channels and the heat transfer becomes worse. For S-shaped fins with a fin angle of 10° , a long fin body creates a long fin tip that separates the flow along the fin body, (e.g. a S-shaped fin design with 10° fin angle and 12.88 mm fin length, as shown in Fig. 13), which increases the pressure drop and enhance the heat transfer simultaneously. In the high-angle-fin group, most of the S-shaped fin designs are the ones with the fin angle of 60° . Short fins are favorable in terms of the thermal effectiveness. However, the pressure drop increases as the fin length decreases. Therefore, we recommend the S-shaped fin channel with 11.6° fin angle and 6.08 mm fin length for the low pressure-drop applications and the one with 60° fin angle and 9.95 mm fin length for the medium-pressure-drop and high-thermal-effectiveness applications.

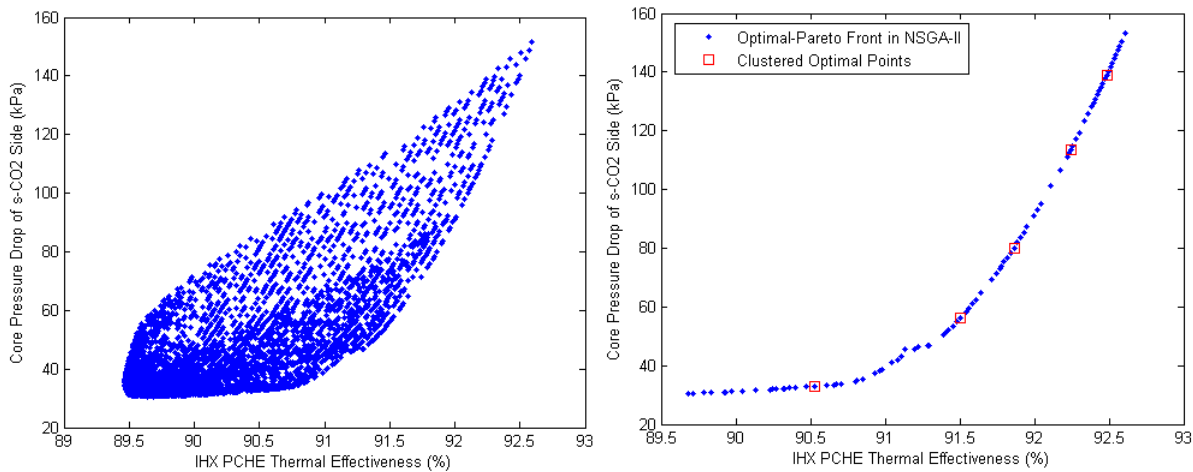


Figure. 11. The Population of 5,000 Solutions in the Design Space (left) and the Optimization Results using NSGA-II and the Clustered Results (right)

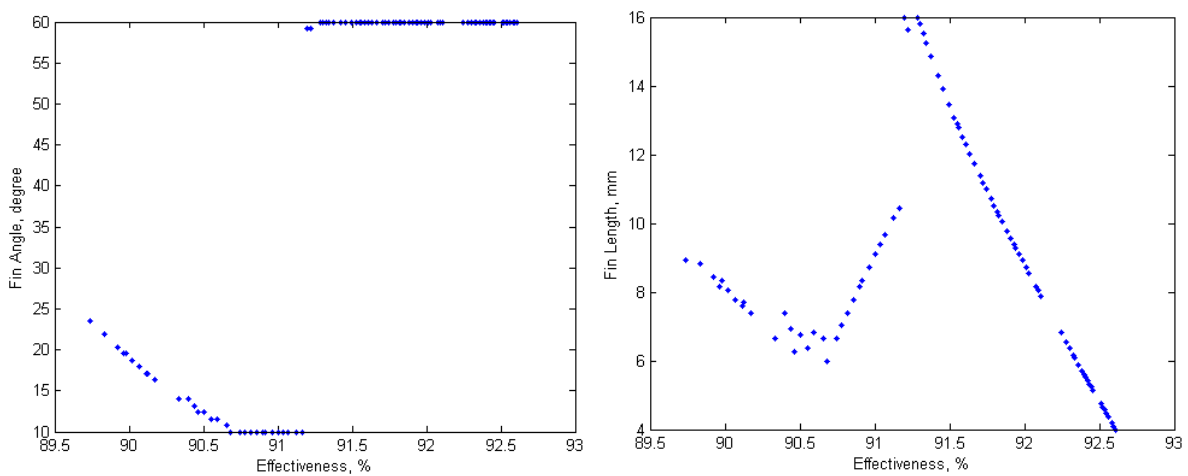


Figure. 12. The Optimization Results using NSGA-II and the Clustered Results

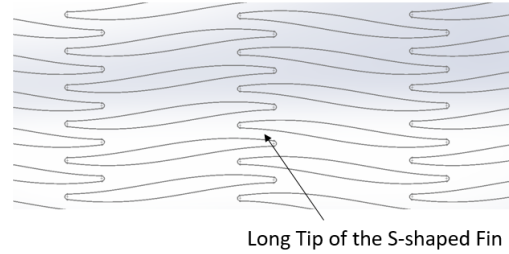


Figure. 13. The Schematic of the S-shaped Fin with 10° Fin Angle and 12.88 mm Fin Length

Table VII. Design Parameters of 5 Clustered Solutions from Optimization.

Item	Symbol	Units	#1	#2	#3	#4	#5
Fin angle	φ	degree	11.6	60.0	60.0	60.0	60.0
Fin length	l_f	mm	6.08	13.35	9.95	6.83	4.94
HX capacity	Q	kW	13.46	13.60	13.66	13.71	13.75
Cold side mass flow rate	q_m	kg/s	0.067	0.084	0.085	0.087	0.089
Cold side inlet temperature	$T_{c,in}$	°C	418.8	418.8	418.8	418.8	418.8
Cold side outlet temperature	$T_{c,out}$	°C	591.6	593.5	594.2	594.9	595.3
Reynolds number	Re	n/a	20000	20000	20000	20000	20000
HX core cold side pressure drop	Δp	kPa	33.04	56.28	80.17	113.46	138.94
Cold side heat transfer coefficient	h	$\text{kW/m}^2\text{-}^\circ\text{C}$	4.538	4.329	4.611	4.931	5.154
Overall heat transfer area	A_s	m^2	0.122	0.154	0.156	0.160	0.163
HX thermal effectiveness	ε	%	90.53	91.51	91.86	92.24	92.48
Number of heat transfer units	NTU	n/a	4.00	4.25	4.35	4.45	4.53

5. Conclusion

S-shaped fin channels were proposed in the literature to address the pressure drop reduction issue in the design of PCHEs for application in s-CO₂ Brayton cycles. To investigate the thermal-hydraulic characteristics of the S-shaped fin channels, a coupling experimental testing system STL is being constructed for testing the prototypic IHX PCHE with S-shaped fin channels. To maximize the heat exchanger thermal effectiveness and minimize the overall pressure drop across the heat exchanger core, a shape optimization of S-shaped fin channels for the prototypic IHX PCHE was carried out using an RSM surrogate model based on CFD simulations results of nine S-shaped fin design models. The optimization procedure was based on one of the widely used MOEAs, NSGA-II. The design variables are selected as the fin angle and fin length, which was shown to strongly affect the thermal-hydraulics of the S-shaped fin channels in the previous parametric studies. In the current study, CFD simulations for 9 S-shaped fin design models were completed, considering the thermal-hydraulic dependence on the fin angle and fin length. The optimization results indicate that the small-fin-angle channels with large fin length are able to reduce the pressure drop while the large-fin-angle channels with small fin length are favorable in increasing the heat exchanger thermal effectiveness. In the future, more design factors need to be taken into account such as the fin arc length and Reynolds number dependence such that the optimization results can be used in broad applications.

6. Acknowledgement

This research is being performed using funding received from the U.S. Department of Energy (DOE) Office of Nuclear Energy's Nuclear Energy University Programs. The authors at the Ohio State University and the University of Wisconsin-Madison appreciate the support.

7. References

1. C.H. Oh, E.S. Kim and M. Patterson, "Design Option of Heat Exchanger for the Next Generation Nuclear Plant", *Journal of Engineering for Gas Turbines and Power*, **132**, 032903 (2010).
2. T. Ishizuka, Y. Kato and T. Ishizuka, "High Performance Printed Circuit Heat Exchanger," *Applied Thermal Engineering*, **27**, pp. 1702-1707 (2007).
3. N. Tsuzuki, Y. Kato, K. Nikitin, N.L. and T. Ishizuka, "Advanced Microchannel Heat Exchanger with S-shaped Fins," *Journal of Nuclear Science and Technology*, **46**, pp. 403-412 (2009).
4. T.L. Ngo, Y. Kato, K. Nikitin and T. Ishizuka, "Heat Transfer and Pressure Drop Correlations of Micro-Channel Heat Exchanger with S-shaped and Zigzag Fins for Carbon Dioxide Cycles," *Experimental Thermal and Fluid Science*, **32**, pp. 560-570 (2007).
5. S.M. Lee, K.Y. Kim and S.W. Kim, "Multi-objective Optimization of a Double-faced Type Printed Circuit Heat Exchanger," *Applied Thermal Engineering*, **60**, pp. 44-50 (2013).
6. K. Deb, *Multi-Objective using Evolutionary Algorithm*, Chapters 2 & 5, John Wiley & Sons, London, UK (2001)
7. R.H. Myers, D.C. Montgomery, *Response Surface Methodology: Process and Product Optimization Using Designed Experiments*, Wiley, New York (1995).
8. E.S. Kim, C.H. Oh and S. Sherman, "Simplified Optimum Sizing and Cost Analysis for Compact Heat Exchanger in VHTR," *Nuclear Engineering and Design*, **238**, pp. 2635-3647 (2008).
9. X., Zhang, X., Sun, R.N., Christensen, and M., Anderson, "Preliminary Structural Assessment of a Printed Circuit Heat Exchanger with S-shaped Fins," *Proceedings of the 16th International Topical Meeting on Nuclear Reactor Thermal Hydraulics (NURETH-16)*, August 30 – September 4, 2015, Chicago, IL, pp. 7673-7686.
10. National Institute of Standards and Technology Chemistry WebBook, <http://webbook.nist.gov> (access in 2015).
11. J.E. Hesselgreaves, *Compact Heat Exchangers – Selection, Design and Operation*, pp. 208, Elsevier Science, Oxford, UK (2001).
12. X. Zhang, X. Sun, R.N. Christensen, M. Anderson and M. Carlson, "Multi-Objective Optimization of a PCHE-Type Intermediate Heat Exchanger Using Genetic Algorithms," accepted by *International Topical Meeting on Advances in Thermal Hydraulics 2016 (ATH'16)*, June 12-16, 2016, New Orleans, LA.